Identification of the Protein Storage Vacuole and Protein Targeting to the Vacuole in Leaf Cells of Three Plant Species[1]

Misoon Park, Soo Jin Kim, Alessandro Vitale, and Inhwan Hwang*

Center for Plant Intracellular Trafficking (M.P., S.J.K., I.H.) and Division of Molecular and Life Sciences (M.P., I.H.), Pohang University of Science and Technology, Pohang, 790–784, Korea; and Istituto di Biologia e Biotecnologia Agraria, Consiglio Nazionale delle Ricerche, 20133 Milano, Italy (A.S.)

Protein storage vacuoles (PSVs) are specialized vacuoles devoted to the accumulation of large amounts of protein in the storage tissues of plants. In this study, we investigated the presence of the storage vacuole and protein trafficking to the compartment in cells of tobacco (*Nicotiana tabacum*), common bean (*Phaseolus vulgaris*), and Arabidopsis leaf tissue. When we expressed phaseolin, the major storage protein of common bean, or an epitope-tagged version of α-tonoplast intrinsic protein (α-TIP, a tonoplast aquaporin of PSV), in protoplasts derived from leaf tissues, these proteins were targeted to a compartment ranging in size from 2 to 5 μm in all three plant species. Most Arabidopsis leaf cells have one of these organelles. In contrast, from one to five these organelles occurred in bean and tobacco leaf cells. Also, endogenous α-TIP is localized in a similar compartment in untransformed leaf cells of common bean and is colocalized with transiently expressed epitope-tagged α-TIP. In Arabidopsis, phaseolin contained N-glycans modified by Golgi enzymes and its traffic was sensitive to brefeldin A. However, trafficking of α-TIP was insensitive to brefeldin A treatment and was not affected by the dominant-negative mutant of AtRab1. In addition, a modified α-TIP with an insertion of an N-glycosylation site has the endoplasmic reticulum-type glycans. Finally, the early step of phaseolin traffic, from the endoplasmic reticulum to the Golgi complex, required the activity of the small GTPase Sar1p, a key component of coat protein complex II-coated vesicles, independent of the presence of the vacuolar sorting signal in phaseolin. Based on these results, we propose that the proteins we analyzed are targeted to the PSV or equivalent organelle in leaf cells and that proteins can be transported to the PSV by two different pathways, the Golgi-dependent and Golgi-independent pathways, depending on the individual cargo proteins.

Plant cells contain multiple types of vacuoles such as the lytic and protein storage vacuoles (PSVs; Paris et al., 1996; Jauh et al., 1998, 1999; Neuhaus and Rogers, 1998). However, the distinctions between the different types of vacuoles may not be as clear as their names indicate. Tonoplast intrinsic proteins (TIPs, a family of aquaporins) have been used as marker proteins for different types of vacuoles (Hoh et al., 1995; Paris et al., 1996; Jauh et al., 1998, 1999; Swanson et al., 1998; Hinz et al., 1999; Jiang et al., 2000). For example, α-TIP and the dark-induced protein isoform of TIP have been shown to localize in the PSV found in seeds and root tip cells, whereas γ-TIP localizes in the tonoplast of the lytic vacuole (Johnson et al., 1989; Hoh et al., 1995; Paris et al., 1996; Jiang et al., 2000). In addition, δ-TIP has been shown to localize at the tonoplast of another type of the vacuole that is generated by wounding or the developmental switches that affect carbon and nitrogen sinks in the leaf cells of soybean (*Glycine max*; Jauh et al., 1998).

These studies clearly demonstrate that multiple types of vacuoles occur not only in a single plant species but also in a single cell.

The biological roles of the lytic vacuole present in most cells and PSVs in seed cells are rather clear (Herman and Larkins, 1999; Marty, 1999). The lytic vacuole is important for maintenance of turgor pressure, storage of metabolites, sequestration of xenobiotic compounds, and digestion of cytoplasmic constituents. In seeds, PSVs store storage and defense proteins (Neuhaus and Rogers, 1998). However, the biological functions of the multiple types of vacuoles in other cell types are not fully understood. Also, the relationship between the different types of vacuoles and the biogenesis and distribution of these organelles in the cell remain elusive. The highly dynamic nature of the vacuole in terms of biological functions makes often difficult to define their exact cellular roles in the cell. The PSVs (Paris et al., 1996; Marty, 1999) or autophagic vacuoles (Aubert et al., 1996) fuse with the lytic vacuole in cells under certain conditions. Also, a new type of vacuoles was generated from existing vacuoles upon environmental changes (Jauh et al., 1998) or during development (Jauh et al., 1999). In an effort to better understand the biogenesis of vacuoles, Di Sansebastiano et al. (2001) showed that acidic (lytic) and neutral (possibly storage) vacuoles are regenerated from the evacu-

olated protoplasts of tobacco (*Nicotiana tabacum*) cells. Also, Jiang et al. (2000, 2001) showed that the crystalloid found within certain PSVs is a membrane-bound compartment resembling lytic vacuoles, providing some further insight into the complexity of vacuolar biogenesis.

An important aspect of vacuole biogenesis regards the trafficking of resident proteins to these compartments. There is vast experimental evidence that proteins destined for the lytic vacuole are first transported from the endoplasmic reticulum (ER) through the Golgi apparatus; clathrin-coated vesicles are then involved in trafficking from the trans-Golgi network (TGN) to the endosome-like prevacuolar compartment. The sorting signals present on plant-soluble proteins destined to lytic vacuoles and the receptor involved seem to be unique to plants, but apart from this important difference, this traffic involves compartments, vesicle coats, and accessory proteins in large part similar to the ones involved in traffic to animal lysosomes and yeast vacuoles (for review, see Vitale and Raikhel, 1999; Bassham and Raikhel, 2000; see also Jin et al., 2001; Kim et al., 2001; Sanderfoot et al., 2001). The mechanisms of protein trafficking to the storage vacuole may instead be exclusive to plant cells (for review, see Müntz, 1998; Vitale and Raikhel, 1999). At least two trafficking pathways to the PSV have been identified: the Golgi-dependent and Golgi-independent pathways (Levanony et al., 1992; Hara-Nishimura et al., 1998; Jiang and Rogers, 1998; Jiang et al., 2000; Toyooka et al., 2000). Many storage proteins, such as the ones of the 7S and 11S class and defense proteins like lectins are transported through the Golgi apparatus and then dense vesicles before being deposited into PSVs. The dense vesicles do not have a clathrin coat. The sorting signals present on PSV proteins are distinct from the ones of lytic vacuolar proteins, but a receptor has not been identified yet. Transient aggregation may play a role in sorting (Saalbach et al., 1991; Holkeri and Vitale, 2001). Electron-dense condensates of the 7S and 11S storage proteins of pea (*Pisum sativum*) can be observed already within the cis-Golgi apparatus, suggesting that the sorting events for these proteins can occur quite early during traffic (Hillmer et al., 2001). The storage globulins in pumpkin (*Cucurbita pepo*) seeds and a Cys proteinase containing a transient ER-retention signal are instead transported to PSVs in a Golgi-independent manner (Hara-Nishimura et al., 1998; Toyooka et al., 2000). These proteins form large aggregates in the ER and are then directed to PSVs by large vesicles, termed precursor-accumulating vesicles or KDEL-vesicles, that directly fuse with PSVs by unknown mechanisms. Wheat storage proteins are also in part delivered to PSVs via a Golgi-independent route (Levanony et al., 1992). There is controversy on whether the Golgi complex is involved in the traffic of the PSV tonoplast protein
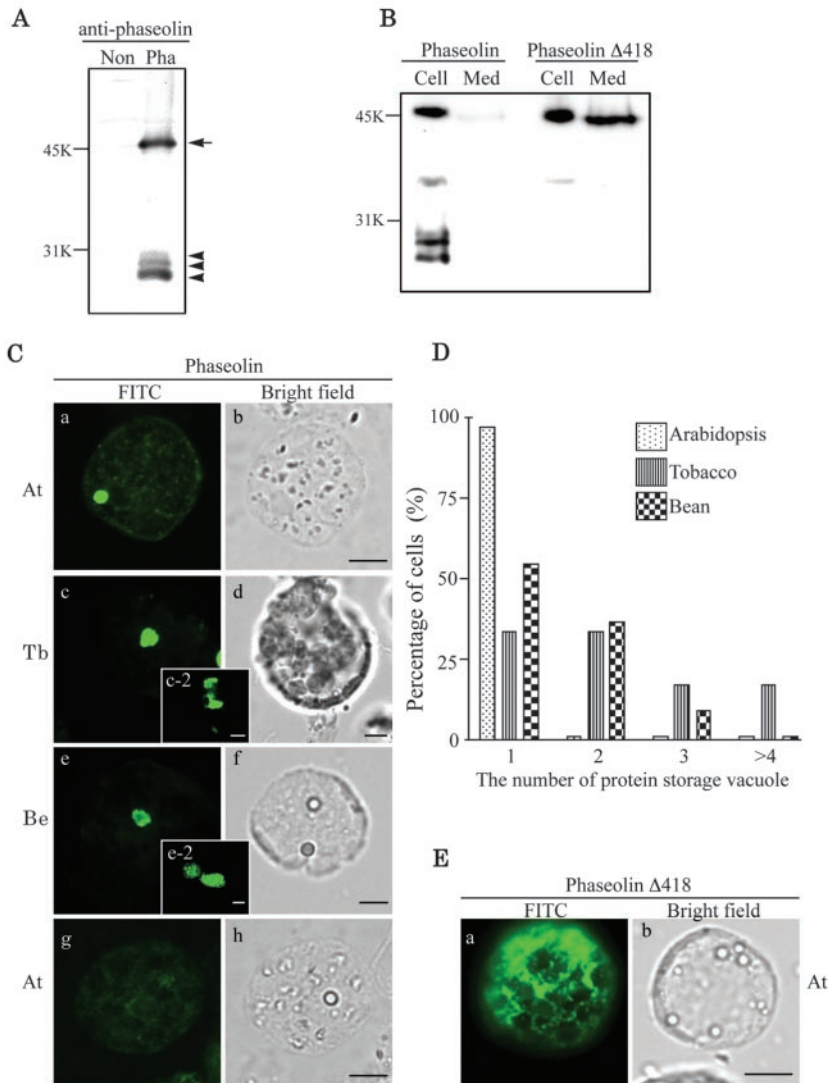
α-TIP (Gomez and Chrispeels, 1993; Hinz et al., 1999).

To gain further insights into the biogenesis of different vacuoles, we investigated the presence of the protein storage vacuole and the targeting of cargo proteins to vacuoles in tobacco, bean (*Phaseolus vulgaris*), and Arabidopsis leaf cells. Here, we present evidence that leaf cells of three plant species have one or multiple PSVs and that proteins can be targeted to the compartment by two different pathways: the Golgi-dependent and Golgi-independent pathways.

RESULTS

Expression and Localization of Phaseolin in Protoplasts of Leaf Cells of Arabidopsis, Tobacco, and Bean

To investigated whether PSVs are also present in the leaf cells of various plant species, we expressed phaseolin, a storage protein found in the seed of the common bean (Müntz, 1998), in protoplasts of Arabidopsis leaf tissues. First, we examined the expression pattern of phaseolin by protein-blot analysis using a polyclonal antiphaseolin antiserum. As shown in Figure 1A, at 24 h after transformation, multiple bands of proteins were detected from protoplasts transformed with the phaseolin construct. The 46-kD band is the expected size of phaseolin (Frigerio et al., 1998). However, we detected three additional bands at the 20- to 25-kD region. These protein bands represent fragmentation products that are produced when phaseolin is sorted to vacuoles in heterologous plants (Bagga et al., 1995; Pedrazzini et al., 1997). To further examine the behavior of phaseolin, we expressed a deletion mutant, phaseolin Δ418, which is missing the C-terminal tetrapeptide that constitutes the vacuolar sorting signal of this storage protein (Frigerio et al., 1998). As shown in Figure 1B, phaseolin Δ418 was secreted into the medium, indicating that, as in tobacco leaf cells (Frigerio et al., 1998), the mutant phaseolin is not sorted to the vacuole and is secreted through the default pathway. In addition, approximately 50% of phaseolin was still present in the cell in its intact form. No vacuolar fragmentation products were detectable, similar to what is observed in leaves of transgenic tobacco plants (Frigerio et al., 1998). These protein-blot analyses of phaseolin strongly suggest that phaseolin may be transported to the vacuole in protoplasts of Arabidopsis leaf cells as in tobacco cells. Therefore, we examined the localization of phaseolin in leaf cells by immunohistochemistry using the antiphaseolin antibody. This time we prepared protoplasts from leaf tissues of three different plant species: Arabidopsis, tobacco, and bean, and we compared the localization of transiently expressed phaseolin. When the protoplasts were transformed with the phaseolin construct, we observed disc patterns of the green fluorescent signals from all three plant species, as

A

anti-phaseolin

Non Pha

B

Phaseolin   Phaseolin Δ418

Cell Med   Cell Med

C

Phaseolin

FITC   Bright field

D

E

Phaseolin Δ418

FITC   Bright field

Figure 1. Expression and localization of phaseolin in leaf protoplasts of three plant species. A, Western-blot analysis of phaseolin in Arabidopsis. Protein extracts were prepared from protoplasts transformed with *phaseolin* (Pha) and untransformed protoplasts (Non) 24 h after transformation and were analyzed by western-blot analysis using an antiphaseolin antibody. Arrow and arrowheads indicate unprocessed and processed forms of phaseolin, respectively. B. Secretion of phaseolin Δ418. Protoplasts were transformed with *phaseolin* or *phaseolin* Δ418. At 24 to 36 h after transformation, protein extracts were prepared from the protoplasts (Cell) and medium (Med). The presence of phaseolin proteins in these protein extracts was detected by western-blot analysis using antiphaseolin antibody. C, Localization of phaseolin in protoplasts of Arabidopsis, tobacco, and bean. Protoplasts derived from leaf tissues of Arabidopsis (At), tobacco (Tb), and bean (Be) were transformed with the phaseolin construct and were fixed 24 to 48 h after transformation. The fixed cells were stained with antiphaseolin antibody followed by fluorescein isothiocyanate (FITC)-labeled anti-rabbit immunoglobulin (Ig) G antibody. As a control for immunostaining, the Arabidopsis protoplasts were treated exactly the same way except that the primary antibody was omitted in g and h. Bar = 20 μm. D, Quantification of the number of discs in a protoplast. The number of the disc as shown in C (a, c, and e) was counted from more than 50 immunostained protoplasts for each plant species. Three identical experiments were performed. E, Localization of phaseolin Δ418. Fixed Arabidopsis protoplasts transformed with phaseolin Δ418 was stained with antiphaseolin antibody followed by FITC-labeled anti-rabbit IgG antibody. Bar = 20 μm. At, Arabidopsis.

shown in Figure 1C (a, c, and e). The pattern is quite different from the large central vacuole of leaf protoplasts that can be highlighted by expressing soluble protein constructs bearing signals for the lytic vacuole in tobacco or Arabidopsis (Di Sansebastiano et al., 2001; Kim et al., 2001). Instead, the pattern shown in Figure 1C is very similar to the one observed in leaf protoplasts of transgenic tobacco that expresses phaseolin (see Fig. 4 in Frigerio et al., 2001). In Arabidopsis cells, approximately 80% of the transformed protoplasts showed the disc pattern. The rest of the cells showed diffuse or punctate staining patterns (data not shown). The percentage of cells demonstrating the disc pattern was slightly higher in tobacco and bean protoplasts (approximately 90%, *n* = 150) than in Arabidopsis cells (approximately 80%, *n* = 150). The size of the disc ranged from 2 to 5 μm. These results, together with data from the protein-blot analysis, strongly suggest that the storage protein phaseolin behaves in the same way in the leaf cells of all three plant species. However, interest-

ingly, the number of discs (Fig. 1C, a, c, and e) in a cell differed depending on the plant species. As shown in Figure 1D, most of the Arabidopsis protoplasts had only a single disc. In contrast, only 35% of tobacco cells showed a single disc, whereas the rest of the cells showed multiple discs in a cell (Fig. 1C, c-2). Interestingly, approximately 18% of tobacco cells had even four or more discs in a cell. In bean cells, the number of discs varied from one to three; approximately 55% of the cells showed a single disc, 35% of the cells showed two discs, and 10% of the cells showed three discs (Fig. 1C, e and e-2). These results suggest that the number of organelles showing the disc pattern is species dependent. As a control, we also examined localization of phaseolin Δ418 present in the cell. As shown in Figure 1E, phaseolin Δ418 present in the cell gave an ER-like network pattern in contrast to the disc pattern observed with wild-type phaseolin, confirming that phaseolin Δ418 is not transported to the PSV. The reticular pattern suggests that most of intracellular phaseolin Δ418 represents

the newly synthesized form of the protein present in the endomembrane system en route to secretion. As we underlined above, a relevant proportion of wild-type phaseolin is also found intact within protoplasts (see Fig. 1A); however, in this case, a reticular pattern is only faintly visible by immunofluorescence (compare Fig. 1C, a, with the control in g). Therefore, in the case of wild-type phaseolin, the intact form may mainly represent the protein that has already reached the PSV but has not yet been fragmented. Also during transient expression in tobacco protoplasts, traffic of phaseolin Δ418 toward secretion seems to be slower than vacuolar traffic of wild-type phaseolin (A. Vitale, unpublished data). The reason for this difference is unknown.

Phaseolin Is Transported through the Golgi Apparatus in Arabidopsis

In bean cotyledons and tobacco leaf cells, the Golgi apparatus mediates the traffic of phaseolin to vacuoles (Chrispeels, 1983; Frigerio et al., 1998). To investigate whether phaseolin is transported through the Golgi apparatus in Arabidopsis as well, we examined its N-glycan moiety. The phaseolin construct used in this study has a single glycan at Asn 252 (Pedrazzini et al., 1997). In bean and tobacco cells, singly glycoylated phaseolin acquires full resistance to in vitro digestion by endo-β-N-acetylglucosaminidase H (endo H) (Frigerio et al., 1998). High-Man glycans present on glycoproteins before they leave the ER are susceptible to endo H; resistance is acquired because of glycan modification operated by Golgi enzymes and therefore is a good indication of traffic through this compartment. First, we examined whether phaseolin is glycosylated in Arabidopsis protoplasts. Protein extracts were prepared from protoplasts expressing phaseolin in the presence and absence of tunicamycin, an inhibitor of glycosylation. The migration pattern of phaseolin was examined by protein-blot analysis. As shown in Figure 2A, the intact form of phaseolin migrated slightly faster in the presence of tunicamycin (Fig. 2A, lane 2) than in the absence of the inhibitor (Fig. 2A, lane 1), indicating that phaseolin is glycosylated in Arabidopsis cells. No phaseolin fragments are detectable in tunicamycin-treated protoplasts, indicating an inhibitory effect on traffic or high susceptibility of the unglycosylated protein to proteases, leading to full degradation during traffic or in vacuoles. Next, we examined the sensitivity of the N-glycan moiety to endo H. As shown in Figure 2A, endo H treatment did not change the mobility of intact or fragmented forms of phaseolin (Fig. 2A, lane 3), suggesting that the N-glycan of phaseolin is modified to the complex type, an indication that it had passed through the Golgi apparatus. As a control for the endo H treatment, we prepared protein extracts from protoplasts expressing phaseolin and a dominant-negative mu-

tant of AtSar1p. In animal and yeast cells, antero-grade trafficking of proteins from the ER for the Golgi complex requires the coat protein complex II (COPII). Sar1p is a small GTPase required for COPII formation. As in the case of animal cells, the dominant-negative AtSar1[H74L] has been shown to inhibit COPII-dependent trafficking of cargo proteins from the ER (Takeuchi et al., 2000; Phillipson et al., 2001; Sohn et al., 2003). When AtSar1[H74L] was coexpressed, no phaseolin fragmentation products were detectable (Fig. 2A, lane 4). Furthermore, endo H treatment caused phaseolin to migrate at the same position of the protein synthesized in the presence of tunicamycin (Fig. 2A, lane 5), indicating that endo H removes the N-glycan from phaseolin. Also, phaseolin gave a network pattern when coexpressed with AtSar1[H74L] (Fig. 2D). Therefore, the protein was not transported beyond the ER. The effect of the dominant-negative GTPase was also tested on the trafficking of the mutated, secreted phaseolin Δ418. Coexpression of AtSar1[H74L] strongly inhibited secretion of phaseolin Δ418 (Fig. 2B). In addition, phaseolin Δ418 gave a network pattern in the presence of AtSar1[H74L] (Fig. 2D). Together, these results indicate that in Arabidopsis protoplasts exit of phaseolin from the ER requires the COPII machinery. Furthermore, the traffic of the mutated phaseolin deprived of the vacuolar sorting signal also requires the COPII machinery. Finally, the observation that intact phaseolin is resistant to endo H digestion (Fig. 2A) indicates that the intact protein has already passed through the Golgi complex, and may have also reached the vacuole, consistently with the immunofluorescence data.

To obtain further insights on phaseolin trafficking, transformed protoplasts were incubated in the presence of brefeldin A (BFA), an inhibitor of ADP-ribosylation factor (Arf1) activity (Lee et al., 2002). Arf1p is involved in the formation of COPI-coated vesicles, which mediate traffic from the ER to the Golgi complex. Inhibition of Arf1p activity by BFA causes redistribution of Golgi proteins into the ER, forming a new ER-Golgi supercompartment, and it also blocks anterograde traffic from the ER and the Golgi complex (Gomez and Chrispeels, 1993; Boevink et al., 1999; Lee et al., 2002; Ritzenthaler et al., 2002). Traffic of phaseolin expressed in BFA-treated protoplasts was probed by protein-blot analysis. As shown in Figure 2C, phaseolin remained intact, indicating that the smaller fragments are generated during trafficking, similar to what has been observed in tobacco protoplasts using a similar BFA sensitivity traffic assay (Pedrazzini et al., 1997). To examine the localization of phaseolin in Arabidopsis in the presence of BFA, protoplasts were fixed and stained with the antiphaseolin antibody. As shown in Figure 2E, phaseolin was detected as a network pattern that may represent the ER or ER/Golgi hybrid detected in the presence of BFA (Ritzenthaler et al., 2002). We
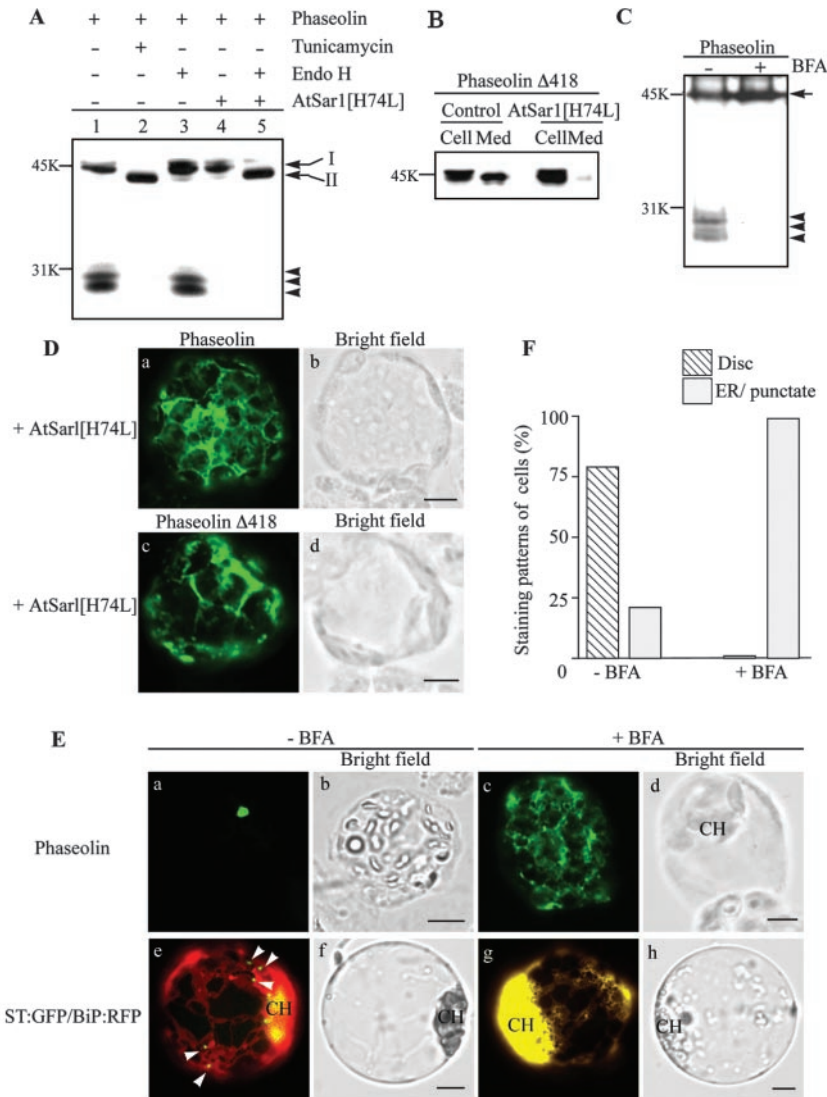
Figure 2. Golgi-dependent trafficking of phaseolin in Arabidopsis protoplasts. A, Western-blot analysis of phaseolin under various conditions. Arabidopsis protoplasts were transformed with *phaseolin* alone or together with *AtSar1[H74L]*. To inhibit glycosylation, tunicamycin (10 μg mL^{-1}) was added to the incubation medium right after transformation and the protoplasts were incubated for 24 h. Protein extracts were prepared from the protoplasts and were treated with endo H. The migration patterns of phaseolin in these protein extracts were analyzed by western-blot analysis using an anti-phaseolin antibody. Bands I and II indicate glycosylated and unglycosylated phaseolin, respectively. Arrowheads indicate fragmented forms of phaseolin. B, Effect of AtSar1[H74L] on the secretion of phaseolin Δ418. Protoplasts were transformed with *phaseolin* Δ418 alone or together with *AtSar1[H74L]*. Protein extracts were prepared from the protoplasts (Cell) and medium (Med) and were analyzed for the presence of phaseolin Δ418 with the antiphaseolin antibody. C, The effect of BFA on the destiny of phaseolin. Protoplasts derived from leaf cells of Arabidopsis were transformed with *phaseolin* and were incubated in the presence (+BFA) or absence (−BFA) of BFA for 24 h. Protein extracts were prepared and analyzed for phaseolin by western-blot analysis. Arrow and arrowheads indicate intact and three fragmented forms of phaseolin, respectively. D, Localization of phaseolin in the presence of AtSar1[H74L]. Protoplasts were transformed with *phaseolin* and *AtSar1[H74L]* or *phaseolin* Δ418 and *AtSar1[H74L]* and localization of phaseolin proteins was detected with antiphaseolin antibody in fixed protoplasts. Bar = 20 μm. E, Localization of phaseolin in the presence of BFA. Arabidopsis protoplasts transformed with *phaseolin* or sialyltransferase (*ST*):*green fluorescent protein* (*GFP*) plus binding protein (*BiP*):*red fluorescent protein* (*RFP*) were incubated in the presence (+BFA) or absence (−BFA) of BFA for 6 to 24 h, and localization of phaseolin was detected by immunohistochemistry using the antiphaseolin antibody followed by FITC-labeled anti-rabbit IgG antibody. ST:GFP and BiP:RFP were detected directly by GFP and RFP signals, respectively, from intact protoplasts. Arrowheads indicate ST:GFP localized at the Golgi apparatus. CH, Chloroplasts. DsRed was used to generated BiP:RFP. Bar = 20 μm. F, Quantification of localization patterns. The number of protoplasts was counted based on the pattern shown in E (a and c) for phaseolin. More than 50 protoplasts were scored at each time and at least three independent experiments were performed. Disc and ER indicate the patterns shown in E (a and c, respectively).

obtained nearly identical network pattern at different time points ranging from 6 h to 24 h (data not shown). As a control, we examined the pattern given by the Golgi-located ST:GFP construct (Lee et al., 2002) in the presence and absence of BFA. In this control experiment, an ER marker was also coexpressed with ST:GFP. The ER marker (BiP:RFP; Jin et al., 2001; Kim et al., 2001) is a fusion between the BiP, the ER-located member of the heat shock protein 70 chaperone family) and RFP. As shown in Figure 2E (e and g), the green punctate staining patterns of ST:GFP, an indication of Golgi localization, was changed to a yellow network pattern, an indication of colocalization with the red pattern given by BiP:RFP and thus of relocation of ST:GFP to the ER-Golgi supercompartments in the presence of BFA (Lee et al., 2002). The strong yellow signals around chloroplasts are caused by the high density of the ER networks that cannot be resolved into individual networks due to the limited resolution we used (Fig. 2E, g). To further confirm this notion, we quantified the protoplasts based on the staining patterns. As shown in Figure 2F, all the phaseolin disc patterns were changed to the ER pattern. These results further support the notion that phaseolin is transported to the final destination through the Golgi apparatus, as observed in transgenic tobaco (Pedrazzini et al., 1997; Frigerio et al., 2001).

α-TIP Is Targeted to the PSV through a Golgi-Independent Pathway

In bean seed cells, phaseolin is targeted to the PSV. However, it is not clear which is the identity of the vacuole where phaseolin is transported in leaf cells of Arabidopsis, tobacco, and bean. One possibility is that phaseolin is transported to the PSV in leaf cells. To address this possibility, we examined whether another PSV protein can be targeted to the same compartment as phaseolin in Arabidopsis cells. Thus, we investigated the targeting of the PSV tonoplast protein α-TIP. We modified α-TIP with the small epitope, hemagglutinin A (HA), to minimize the disruption of the native protein structure and we expressed it in Arabidopsis protoplasts. Arabidopsis protoplasts were transformed with α-TIP:HA, and protein extracts were prepared from the transformed protoplasts. Expression of α-TIP:HA was first examined by protein-blot analysis using an anti-HA antibody. As shown in Figure 3A, the antibody specifically detected a protein band at the 29-kD position, a calculated M_r of α-TIP:HA, from the protein extracts obtained from protoplasts transformed with α-TIP:HA but not from the protein extracts obtained from untransformed protoplasts.

To determine the localization of α-TIP:HA, protoplasts were cotransformed with α-TIP:HA together with phaseolin. As shown in Figure 3B, α-TIP:HA was depicted in the same disc pattern observed with phaseolin, as detected by immunostaining using the anti-HA antibody. When quantified, the percentage of cells showing the disc pattern was 60% (Fig. 3D). Furthermore, α-TIP at the disc pattern colocalized with phaseolin (95% overlap, $n = 90$), suggesting that α-TIP:HA may be targeted to the PSV in Arabidopsis. In addition, 40% of protoplasts expressing α-TIP:HA gave nondisc patterns such as punctate staining pattern, network-like patterns, and plasma membrane patterns (data not shown). However, in these protoplasts, phaseolin was still present as disc patterns (data not shown). These results suggest that the nondisc pattern observed with α-TIP is not due to lack of the PSV in the protoplasts. The difference in the targeting efficiency of phaseolin and α-TIP:HA to what appears to be the PSV is not clearly understood. We next examined whether it is transported to the PSV through the Golgi apparatus. To address this question, we examined trafficking of α-TIP:HA in the presence of BFA. As shown in Figure 3C, α-TIP:HA gave the disc pattern in the presence of BFA at various time points from 6 to 24 h, indicating that BFA does not affect trafficking of α-TIP:HA to the PSV. In addition, the targeting efficiency of α-TIP:HA to the PSV was not changed in the presence of BFA (Fig. 3D). These results strongly suggest that trafficking of α-TIP:HA to the PSV is independent of the Golgi apparatus. In what appear to be untransformed cells, we did not observe any detectable level of FITC, TRITC, or GFP signals (Fig. 3B, a–d, arrows). Next, we performed colocalization of α-TIP:HA with ST:GFP to examine whether α-TIP:HA is detected at the Golgi apparatus. Protoplasts were cotransformed with α-TIP:HA and *ST:GFP*, and localization of these proteins was examined by immunohistochemistry using anti-HA antibody. As shown in Figure 3E, the red fluorescent signal of α-TIP:HA was not detectable at the Golgi apparatus, indicated by ST:GFP at the condition we used. This result is consistent with the notion that α-TIP:HA is transported to the Golgi-independent pathway.

However, the data above do not provide conclusive evidence for Golgi-independent trafficking of α-TIP:HA. To obtain unequivocal evidence for Golgi-independent trafficking of α-TIP, we examined the glycosylation pattern of overexpressed α-TIP:HA in protoplasts. The Asn-linked glycosylation pattern provides a convenient indication of protein passage through the Golgi apparatus. Golgi-localized glycan-modifying enzymes produce complex type N-glycans that are resistant to endo H, whereas ER-type glycans are sensitive to endo H (Jiang and Rogers, 1998; Nebenfuhr et al., 2002; Ritzenthaler et al., 2002; Sohn et al., 2003). To further confirm the Golgi-independent trafficking of α-TIP, we examined the glycosylation pattern of α-TIP. Although amino acid sequence analysis of α-TIP revealed that it has a potential N-glycosylation site (N78), tunicamycin treatment did not affect the mobility of α-TIP:HA
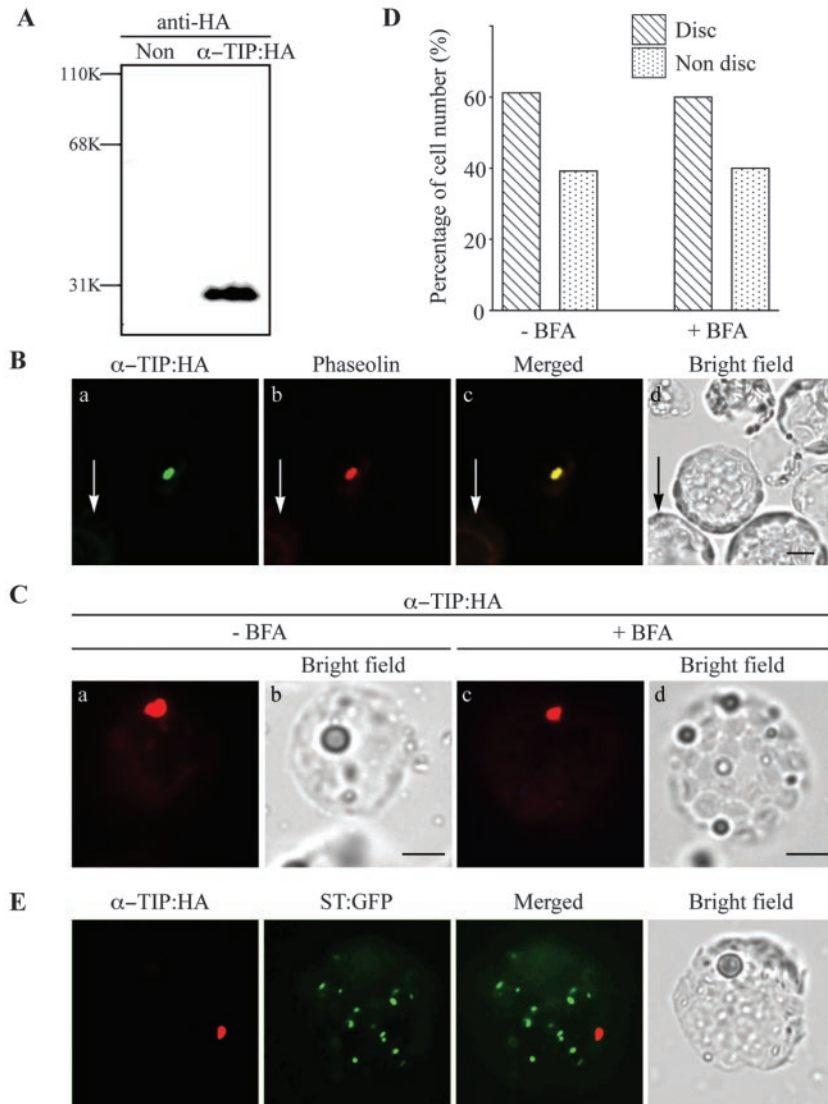
Figure 3. Localization of α-TIP tagged with HA. A, Expression of α-TIP:HA. Arabidopsis protoplasts were transformed with α-TIP:HA and protein extracts were prepared from the transformed protoplasts 24 h after transformation. α-TIP:HA was detected by western-blot analysis using a monoclonal anti-HA antibody. Non, Protein extracts obtained from untransformed protoplasts. B, Localization of reporter proteins. Arabidopsis protoplasts were cotransformed with α-TIP:HA plus *phaseolin* and were fixed with paraformaldehyde 24 to 48 h after transformation. α-TIP:HA was treated with anti-HA antibodies followed by FITC-labeled anti-rat IgG antibody. Phaseolin was detected with antiphaseolin antibody followed by tetramethylrhodamine B isothiocyanate (TRITC)-labeled anti-rabbit IgG antibody. Arrows indicate untransformed cells used as controls. C, The effect of BFA on the localization of α-TIP:HA. Arabidopsis protoplasts transformed with α-TIP:HA were incubated in the presence (+BFA) or absence (−BFA) of BFA and were fixed 48 h after transformation. The localization of α-TIP:HA was detected using anti-HA antibody followed by TRITC-labeled anti-rat IgG antibody. Bar = 20 μm. D, Quantification of localization patterns. The numbers of protoplasts were counted based on the pattern of TRITC. Protoplasts (n = 50–100) were scored at each time and at least three independent experiments were performed. Disc indicates the protoplasts with the TRITC pattern shown in B (a). Nondisc indicates protoplasts with the TRITC pattern other than in B (a). The nondisc patterns include the ER pattern (network pattern), punctate staining pattern, and a minor portion of the lytic vacuolar pattern. E, Lack of colocalization of α-TIP:HA with ST:GFP. Protoplasts were transformed with α-TIP:HA plus *ST:GFP*. Protoplasts were fixed and stained with anti-HA antibody. GFP signals were directly observed on the fixed protoplasts. Bar = 20 μm.

(Fig. 4A), indicating that it is not glycosylated. Thus, we modified α-TIP by inserting the phaseolin C-terminal region (from amino acid positions 226–284) with an N-glycosylation site in the loop between transmembrane domains 5 and 6 (Fig. 4B). First, we examined expression and localization of α-TIP:gly:HA in protoplasts. Protein extracts were prepared from protoplasts transformed with α-TIP:gly:HA and were analyzed by western blotting. As shown in Figure 4D, a 40-kD protein band that was larger than the size of α-TIP:HA was specifically detected from protein extracts obtained from protoplasts transformed with α-TIP:gly:HA (Fig. 4D, lane 2), confirming that the modified protein is expressed in Arabidopsis protoplasts. To confirm that the modified α-TIP:gly:HA is targeted to the PSV as observed with α-TIP:HA, α-TIP:gly:HA was introduced into protoplasts and its localization was examined by immunohistochemistry using anti-HA antibody. As shown in Figure 4C, α-TIP:gly:HA gave a disc pat-

tern, indicating that α-TIP:gly:HA is targeted to the PSV as a modified form. Furthermore, in the presence BFA, α-TIP:gly:HA gave the same disc pattern as observed with α-TIP:HA. These results strongly suggest that α-TIP:gly:HA is transported to the PSV as the modified version. Next, we examined whether α-TIP:gly:HA is glycosylated in Arabidopsis protoplasts. α-TIP:gly:HA was expressed in the presence and absence of tunicamycin. As shown in Figure 4D, tunicamycin caused α-TIP:gly:HA to migrate faster in the gel (Fig. 4D, lane 3) compared with the untreated control (Fig. 4D, lane 2), indicating that α-TIP:gly:HA is glycosylated in Arabidopsis protoplasts. We next examined whether the N-glycan moiety of α-TIP:gly:HA is sensitive to endo H. As shown in Figure 4C (lane 4), endo H-treatment caused majority of α-TIP:gly:HA to migrate faster in the gel, indicating that the N-glycan of α-TIP:gly:HA is sensitive to endo H, an indication of the ER type. This result strongly suggests that α-TIP:gly:HA is not exposed to
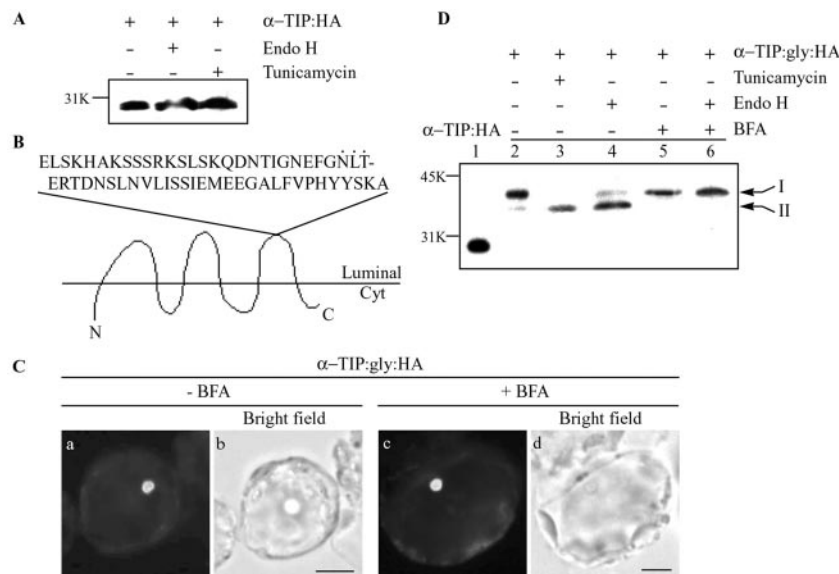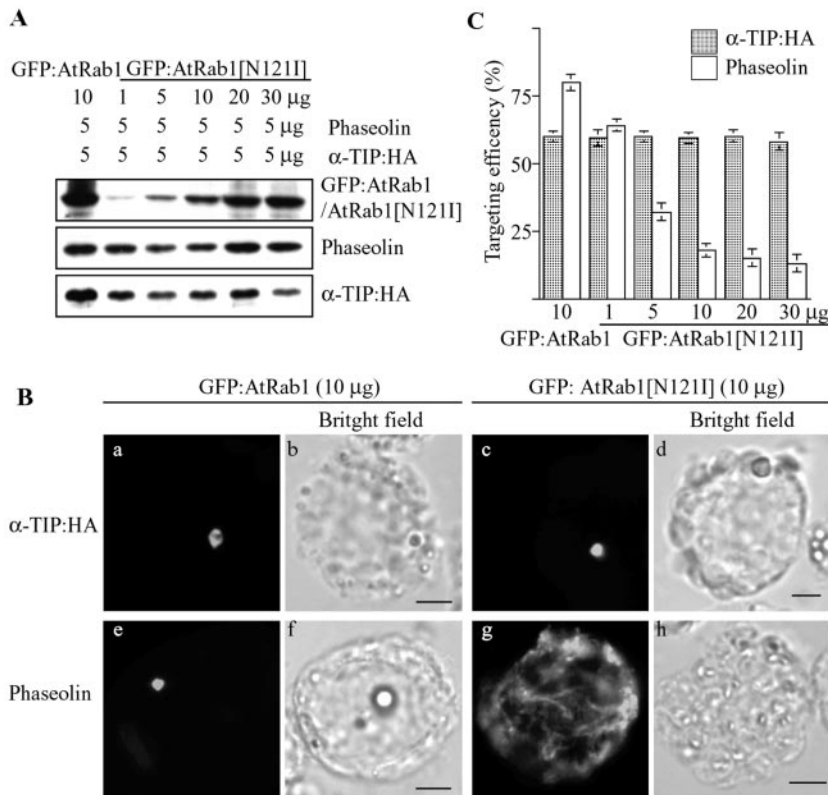
Figure 4. α-TIP:gly:HA is transported to the PSV in protoplasts. A, No glycosylation of α-TIP:HA. Protein extracts were prepared from the protoplasts transformed with α-TIP:HA 36 h after transformation. The protein extracts were fractionated by SDS/PAGE without (Con) or with endo H treatment (Endo H). Also, protein extracts were prepared from protoplasts treated with tunicamycin after transformation (Tun). α-TIP:HA was detected with the anti-HA antibody. B, A scheme of α-TIP:gly: HA. The C-terminal region of phaseolin from amino acid positions 226 to 284, which contains an N-glycosylation site (denoted by dots), was inserted in the loop between transmembrane domains 5 and 6. Cyt, Cytosol. C, Localization of α-TIP:gly:HA. Protoplasts transformed with α-TIP:gly:HA were incubated in the presence and absence of BFA for 6 to 24 h and localization of α-TIP:gly:HA was examined by immunohistochemistry using anti-HA antibody. Bar = 20 μm. D, Western-blot analysis of α-TIP:gly:HA. Protoplasts transformed with α-TIP:HA or α-TIP:gly:HA were incubated in the presence and absence of tunicamycin (10 μg mL^{-1}) for 24 h or in the presence and absence of BFA (25 μg mL^{-1}) for 24 h. Protein extracts were prepared from protoplasts and were analyzed by western-blot analysis using anti-HA antibody. Also, protein extract treated with endo H was included in western-blot analysis. Bands I and II indicate glycosylated and unglycosylated forms, respectively, of α-TIP:gly:HA.

Golgi-localized glycan-modifying enzymes. However, it is possible that the ER type of the N-glycan is due to its inaccessibility to the Golgi-localized modifying enzymes during traffic through the Golgi apparatus. We examined whether the N-glucans of α-TIP:gly:HA can be modified to the endo H-resistant form by the Golgi-localized modifying enzymes. The Golgi-localized glycan-modifying enzymes can be brought to the ER or ER/Golgi hybrid structure when the Golgi apparatus is disassembled by BFA (Ritzenthaler et al., 2002). Protoplasts transformed with α-TIP:gly:HA were incubated in the presence of BFA. Subsequently protein extracts were prepared and treated with endo H. As shown in Figure 4D, endo H treatment did not change the migration pattern of α-TIP:gly:HA present in the protein extracts obtained from protoplasts incubated with BFA (lane 6), strongly indicating that the N-glycan of α-TIP:gly:HA can be modified to the complex type by the Golgi-localized modifying enzymes when they are brought to the ER by BFA treatment. Thus, the fact that α-TIP:gly:HA targeted to the PSV has the ER-type but not the Golgi-type N-glycan moiety strongly suggests that α-TIP does not pass through the Golgi apparatus when it is transported to the PSV in Arabidopsis leaf cells.

Trafficking of α-TIP:HA Is Independent of AtRab1 and AtSec23

To obtain additional evidence for Golgi-independent trafficking of α-TIP:HA, we examined whether AtRab1 is involved in trafficking of α-TIP to the storage vacuole. AtRab1 plays a critical role in ER-to-Golgi trafficking in Arabidopsis (Batoko et al., 2000). The dominant-negative mutant, AtRab1[N121I], has been shown to inhibit trafficking of cargo proteins to the Golgi apparatus. We examined whether AtRab1[N121I] inhibits trafficking of α-TIP:HA to the storage vacuole. Phaseolin was used as a positive control. Protoplasts were transformed with α-TIP:HA and phaseolin together with various amounts of GFP: AtRab1[N121I] or wild-type GFP:AtRab1. The expression of GFP:AtRab1[N121I], phaseolin, and α-TIP:HA was examined by western-blot analysis using anti-GFP, anti-phaseolin, or anti-HA antibodies, respectively. As shown in Figure 5A, these proteins were expressed in protoplasts. Furthermore, the expression level of GFP:AtRab1[N121I] gradually increased, as did the amount of GFP:AtRab1[N121I]. We next examined whether GFP:AtRab1[N121I] inhibits trafficking of α-TIP:HA and phaseolin to the PSV. As shown in Figure 5B (c and g), in the presence of GFP:

AtRab1[N121I], the majority of α-TIP:HA gave a disc pattern, whereas phaseolin presented a network pattern. As a control, we examined the effect of GFP:AtRab1 on the trafficking of α-TIP:HA and phaseolin. As expected, GFP:AtRab1 did not affect the trafficking of either protein (Fig. 5B, a and e). Next, we quantified the targeting efficiency of both proteins based on their staining patterns. The targeting efficiency of phaseolin gradually decreased as the amount of GFP:AtRab1[N121I] increased. When *phaseolin* was cotransformed with 30 μg of *GFP:AtRab1[N121I]*, the targeting efficiency of phaseolin was reduced to 13%. In contrast, the targeting efficiency of α-TIP:HA was not affected by GFP:AtRab1[N121I] even when 30 μg of DNA was used for transformation. These results clearly indicate that α-TIP:HA may be transported by an AtRab1-independent trafficking pathway.

To further support that α-TIP:HA and phaseolin are transported by two different pathways, we examined trafficking of both proteins in the presence of overexpressed AtSec23, a component of COPII vesicles (Movafeghi et al., 1999). Previously, it has been shown that overexpression of Sec23 causes disorganization of the ER-Golgi intermediate compartment and Golgi apparatus and inhibits anterograde trafficking (Tani et al., 1999). The overexpressed Sec23 may cause premature hydrolysis of GTP bound to Sar1 through the GAP activity of Sec23. Phaseolin or α-TIP:HA was cotransformed with increasing amounts of AtSec23 tagged with a small T7 epitope at its N terminus. As expected, the amount of AtSec23 detected with the anti-T7 antibody increased with the amount of introduced DNA (Fig. 6A). Under this condition, we examined the targeting efficiency of phaseolin and α-TIP:HA. In the presence of AtSec23, phaseolin gave a network pattern as observed in the presence of AtRab1[N121I] (Fig. 6B). The percentage of cells with the network pattern increased proportionally with the increase in the level of T7:AtSec23 (Fig. 6C), indicating that trafficking of phaseolin is strongly inhibited by overexpressed AtSec23. In contrast, the percentage of the disc pattern of α-TIP:HA remained nearly the same regardless of the amount of T7:AtSec23 expressed in protoplasts, suggesting that AtSec23 is not involved in trafficking of α-TIP:HA. This result further supports the notion that α-TIP:HA is transported to the PSV through the Golgi-independent pathway.

Untransformed Leaf Cells of Common Bean Contain the PSV

The above data clearly demonstrated that transformed protoplasts contain the PSV where α-TIP and phaseolin are transported by two different trafficking pathways. However, it is not clear whether the PSV is also present in untransformed leaf cells. One possibility is that exogenously expressed PSV proteins may induce formation of the PSV in leaf cells. To address this question, we examined the presence of the PSV in untransformed leaf cells by immunohistochemistry using a polyclonal anti-α-TIP antibody

Figure 6. Overexpressed T7:AtSec23 inhibits trafficking of phaseolin but not α-TIP:HA to the PSV. A, Western-blot analysis of transiently expressed proteins. Protoplasts were transformed with the indicated amounts of each construct. Protein extracts were prepared from transformed protoplasts and transiently expressed proteins were detected by western-blot analysis using anti-GFP, antiphaseolin, or anti-T7 antibodies. R6, An empty vector used as a control. B, Localization of α-TIP and phaseolin. Protoplasts were transformed with the indicated constructs and were stained with anti-HA (α-TIP:HA) or antiphaseolin (phaseolin) antibodies. Bar = 20 μm. C, Quantification of targeting efficiency. Immunostained protoplasts were counted based on localization patterns of α-TIP and phaseolin. The disc pattern shown in a or c was taken to indicate targeting to the PSV. Three independent transformations were performed, and 200 immunostained cells were counted each time. Error bars indicates standard deviation.
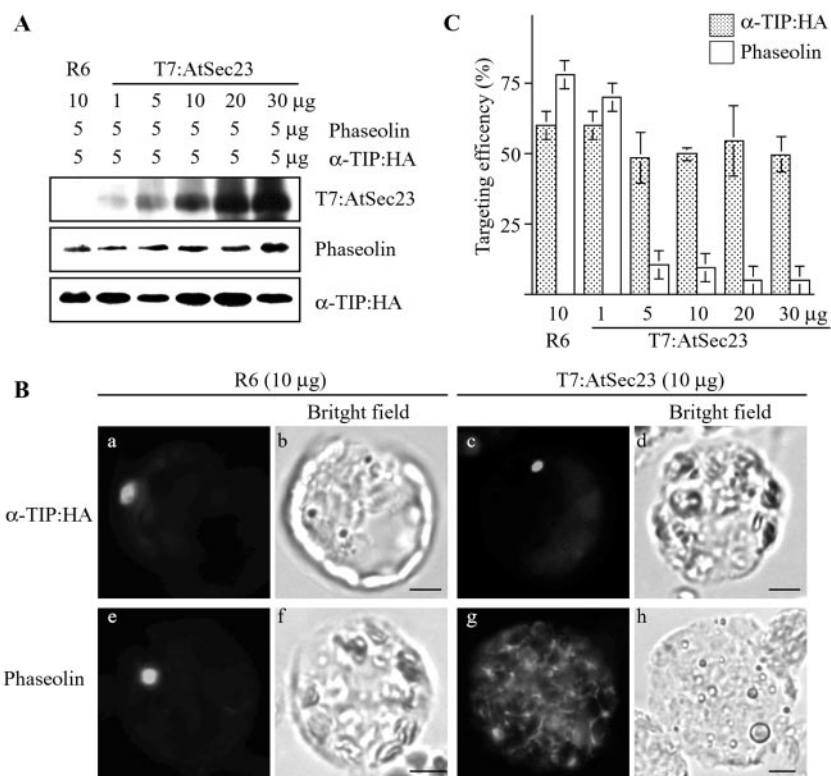
raised against a C-terminal region of common bean α-TIP. α-TIP is an endogenous protein localized at the PSV in various plant species (Johnson et al., 1989; Hoh et al., 1995; Paris et al., 1996; Jiang et al., 2000). Protein extracts were prepared from seeds, cotyledon, and leaf tissues and were analyzed by western-blot analysis using anti-α-TIP antibody. As shown in Figure 7B, a protein at 29 kD was specifically detected in all samples, indicating that α-TIP is expressed in all tissues we examined. However, the expression level was highest in seeds followed by cotyledons as expected. Next, we examined localization of endogenous α-TIP in various tissues. Interestingly, endogenous α-TIP gave two different staining patterns in cotyledons: one with numerous small discs and the other with a few large discs (Fig. 7C, a and c). In true leaves, α-TIP also gave a disc pattern (Fig. 7C, e, g, and i). However, the number of discs in a cell was drastically reduced; majority of young true leaves contain two discs and old true leaves contain only one disc. This result strongly suggests that untransformed true leaf cells also contain the PSV, although the number of the PSV is reduced to one or two depending on the stage of the leaf. We next examined whether untransformed Arabidopsis leaf cells also contain the PSV. To address this, we examined whether the anti-α-TIP antibody crossreacts with Arabidopsis α-TIP. Protein extracts were prepared from Arabidopsis leaf tissues and were used for western-blot analysis with the anti-α-TIP. The anti-α-TIP antibody detected a weak band at the position of α-TIP from Arabidopsis leaf extracts only when we overloaded Arabidopsis protein extracts on an SDS gel or overexposed the western blot. However, at this condition, the anti-α-TIP antibody detected many other proteins in the Arabidopsis leaf extracts (data not shown). Thus, as an alternative, we examined expression of α-TIP in Arabidopsis leaf cells by a reverse transcription (RT)-coupled PCR approach. RT/PCR analysis was performed using total RNA prepared from seeds and leaf cells using α-TIP-specific primers. As a control, expression of γ-TIP was also examined. As shown in Figure 8, an α-TIP-specific band of 600 bp fragment was detected in seeds (Fig. 8, lane 1) and leaf tissues (Fig. 8, lane 3), indicating that α-TIP is expressed in leaf cells as observed in seeds. This result strongly suggests that the PSV may also be present in untransformed Arabidopsis leaf cells, as observed in common bean leaves.

Transiently Expressed α-TIP:HA Colocalizes with Endogenous α-TIP in Bean Leaf Cells

We next examined whether α-TIP:HA is transported to the PSV where endogenous α-TIP has been found to localize. Protoplasts obtained from leaf cells of common bean were transformed with α-TIP:HA, and localization of transiently expressed α-TIP:HA and endogenous α-TIP was examined by immunohistochemistry using anti-HA and anti-α-TIP antibodies, respectively. As shown in Figure 9, the green fluorescence of α-TIP:HA closely overlapped the red
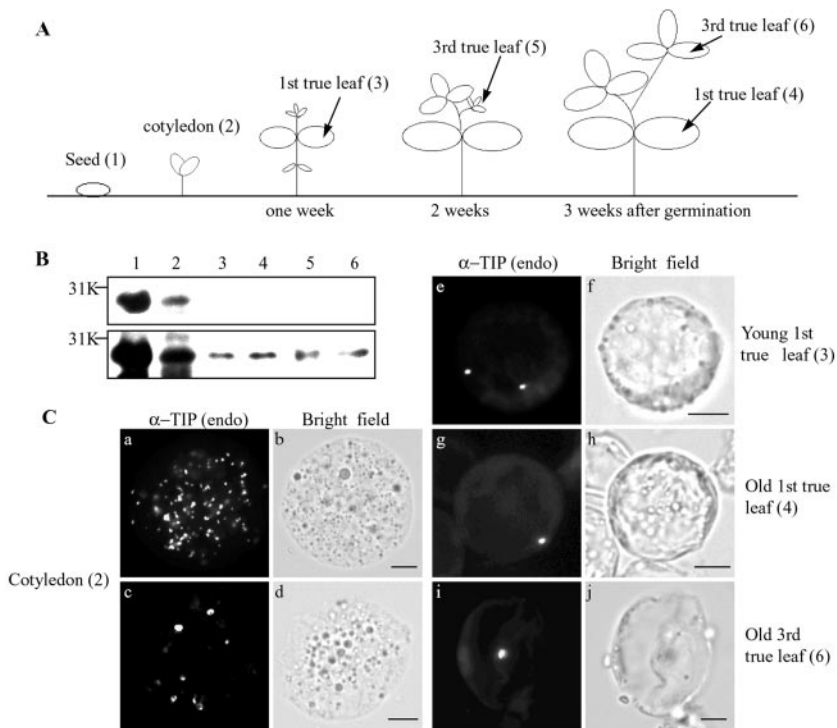
Figure 7. PSVs are present in untransformed leaf cells of common bean. A, Schemes of leaf tissues used in experiments. B, Western-blot analysis of endogenous α-TIP. Protein extracts were prepared from seeds (lane 1), cotyledons (lane 2), and leaf tissues (lanes 3–6) and were analyzed by western-blot analysis using anti-α-TIP antibody. The amount of total proteins loaded was 10 and 50 μg for top and bottom panels, respectively. The numbers are the same as in A. C, Localization of endogenous α-TIP. Protoplasts were prepared from the indicated bean tissues and were immunostained with anti-α-TIP antibody [α-TIP (endo)] after fixation. The numbers are the same as in A. Bar = 20 μm.

fluorescence of endogenous α-TIP, indicating that transiently expressed α-TIP:HA and endogenous α-TIP are targeted to the same compartment in protoplasts.

DISCUSSION

PSV in Leaf Cells

PSVs were originally identified in the reservoir cells of seed tissues, but were later detected in root tips in a variety of different plant species as well (for review, see Neuhaus and Rogers, 1998; Herman and Larkins, 1999). Although possibly many, if not all, young plant cells possess vegetative vacuoles and PSVs (Paris et al., 1996), it is unknown how widely PSVs or similar organelles are present in the differentiated cells of plant tissues. In this study, we investigated the presence of PSV in the cells of leaf tissues by examining the localization of phaseolin and of α-TIP tagged with HA in the protoplasts derived from the leaf tissues of three plant species: Arabidopsis, tobacco, and common bean. The storage protein phaseolin and the aquaporin α-TIP are naturally found in the lumen and the tonoplast, respectively, of PSVs in cotyledonary cells of common bean (Bollini and Chrispeels, 1978; Johnson et al., 1989). In addition, when phaseolin was expressed in transgenic tobacco under a constitutive promoter, it was sorted to the vacuole in leaf cells and was present as protein body-like aggregates (Frigerio et al., 1998; Frigerio et al., 2001). When these proteins are expressed in protoplasts derived from leaf tissues of three different plant species, they were targeted to

the same compartment and detected as disc patterns, strongly suggesting that the disc may represent the PSV. The size of the organelle depicted as the disc pattern ranged from 2 to 5 μm in all three plant species. The most strong support for the notion that the disc represents the PSV came from the observation that untransformed bean leaf cells also gave a disc pattern when immunostained with the PSV-specific α-TIP antibody. Furthermore, transiently expressed α-TIP:HA colocalized with endogenous α-TIP at the PSV. However, the number of organelles differed among the three plant species. In most cases, Arabidopsis cells had only one, and rarely two, of these organelles. In contrast, tobacco and bean cells contained variable numbers of the organelle ranging
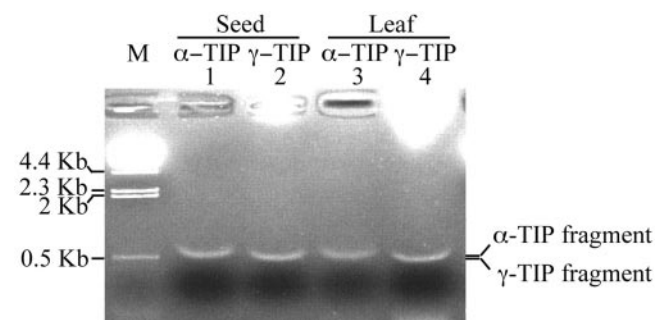
Figure 8. α-TIP is expressed in leaf tissues of Arabidopsis. Total RNA isolated from seeds or leaf tissues was used for RT-PCR analysis and PCR products were analyzed by an agarose gel. As a control, γ-TIP was included in the analysis. The products were sequenced to confirm the identity. The α- and γ-TIP-specific PCR fragments are indicated.

Figure 9. Colocalization of endogenous α-TIP with transiently expressed α-TIP:HA. Protoplasts prepared from leaf cells of common bean were transformed with α-TIP:HA and localization of proteins was examined at 24 h after transformation. Endogenous α-TIP [α-TIP (endo)] and transiently expressed α-TIP:HA (α-TIP:HA) were detected with anti-α-TIP and anti-HA antibodies, respectively. Bar = 20 μm.
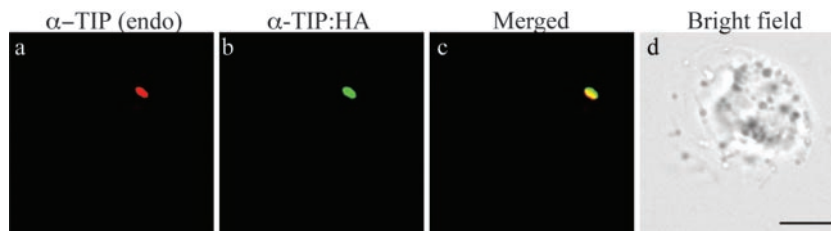
from one to five. Tobacco leaf cells tended to have more of these organelles than the other two plant species. The significance of the difference in the number of the organelle in the plant species is currently unclear.

The biological role of the PSV in seed reservoir cells is rather clear; the PSV contains storage proteins for later use during germination. However, the presence of the PSV or equivalent organelle in leaf cells is rather intriguing. The biological role of this organelle in leaf cells is not clear at present. Lipooxygenase has been shown to be stored in the PSV in leaf cells for the temporary storage of nitrogen during vegetative growth (Tranbarger et al., 1991). We reported here that the biogenesis of this compartment in leaves seems very similar, if not identical to that in seeds, following at least two distinct protein biosynthetic routes. One possible role of the PSV may be to store a large amount of proteins required for the defense response. In fact, chitinase and glucanase, the two well known pathogenesis-related proteins, are known to be targeted to the PSV (Neuhaus and Rogers, 1998). When a leaf cell is attacked by a pathogen, the stored pathogenesis-related proteins may be released to digest the cell wall of the infecting pathogen. However, further studies are necessary to define the exact role of the PSV in leaf cells.

Traffic of PSV Proteins

Phaseolin synthesized in Arabidopsis protoplasts is fully resistant to in vitro digestion with endo H. Furthermore, BFA treatment inhibited delivery of phaseolin to the PSV and caused accumulation within the ER. These results are quite similar to the ones obtained with phaseolin expressed in tobacco (Pedrazzini et al., 1997; Frigerio et al., 1998; Frigerio et al., 2001) and they indicate that phaseolin is transported through the Golgi complex in Arabidopsis, as in common bean cotyledons and tobacco leaf cells. We also showed that coexpression of the dominant-negative GTPases AtSar1[H74L] inhibits exit of phaseolin from the ER, indicating that traffic of phaseolin is dependent on the COPII machinery. It has been previously reported that the dominant-negative GTPase inhibits traffic of GFP fusions targeted to the Golgi complex or lytic vacuoles in tobacco and Arabidopsis cells (Takeuchi et al., 2000) and of two barley (*Hordeum vulgare*) proteins: α-amylase, which is a constitutively secreted protein,

and phytepsin, which is an aspartic protease present in both types of vacuoles in barley root tips and has an unusual vacuolar-sorting determinant (Phillipson et al., 2001; Törmäkangas et al., 2001). Our results extend these observations to a seed storage protein and support the hypothesis of a general role of COPII in mediating ER-to-Golgi traffic in plant cells. This hypothesis is further strengthened by our observation that secretion of phaseolin Δ418 is also inhibited by AtSar1[H74L]. However, it has been shown that traffic of a mutated, secreted form of phytepsin deprived of its vacuolar-sorting signal cannot be inhibited by coexpression of Sar1[H74L] or overexpression of Sec12p, which is another way to inhibit COPII-mediated ER exit (Törmäkangas et al., 2001). This was tentatively explained by hypothesizing the presence of a COPII-independent ER exit route (Törmäkangas et al., 2001), may be coincident to the Golgi-independent route followed by α-TIP. Whatever the explanation, our results indicate that vacuolar-sorting signal-dependent exit at the ER is not a general feature of plant vacuolar proteins and that the view that ER-to-Golgi traffic and vacuolar sorting are independent events seems to hold for phaseolin.

There is evidence that in seed storage tissues, PSV can also be reached by bypassing the Golgi complex. Large vesicles, sometimes termed precursor accumulating vesicle or KDEL vesicle, can leave the ER incorporating certain storage proteins and proteases that have been condensed within the ER lumen; these vesicles can eventually directly deliver their content into PSVs (Levanony et al., 1992; Hara-Nishimura et al., 1998; Toyooka et al., 2000). Furthermore, the bean PSV tonoplast protein α-TIP is transported to the vacuole through a BFA-insensitive pathway when expressed in tobacco leaf protoplasts (Gomez and Chrispeels, 1993). We have shown here that in Arabidopsis protoplasts traffic of HA-tagged α-TIP is BFA insensitive and leads to the same type of vacuole that accumulates phaseolin. In support of this notion is the traffic of a modified glycosylated form of α-TIP (α-TIP:gly:HA) to the PSV. The N-glycan moiety of α-TIP:gly:HA was sensitive to endo H, which indicates that α-TIP:gly:HA is not transported through the Golgi apparatus. Also, its traffic to the PSV is insensitive to BFA. Furthermore, the dominant-negative mutant of AtRab1 did not inhibit trafficking of α-TIP:HA to the PSV. AtRab1 plays a critical role in the ER for Golgi trafficking, which was confirmed by the fact that the dominant-negative mutant of

AtRab1 strongly inhibited trafficking of phaseolin to the PSV. Furthermore, the effect of overexpressed AtSec23, a component of COPII vesicles, on the trafficking of phaseolin and α-TIP:HA to the PSV was nearly identical to that of AtRab1[N121I]. These results together further strengthen our notion that α-TIP:HA is transported to the PSV through the Golgi-independent pathway. However, we cannot completely rule out the possibility that α-TIP is transported through the Golgi complex. It is possible that a COPII-independent pathway from the ER to the Golgi exists and that exit from the Golgi complex could be before resistance to Endo H is conferred. Interestingly, previous studies also showed that anti-α-TIP antibody specifically detects α-TIP at the Golgi apparatus as well as at dense vesicles. The dense vesicles are thought to be derived from the TGN and to be involved in delivery of cargo molecules from the TGN to the PSV (Hinz et al., 1999; Hillmer et al., 2001). These results suggest that α-TIP is transported by the Golgi-dependent pathway. To reconcile these two contradictory results, we hypothesize that α-TIP may be transported to the PSV through the Golgi-dependent and Golgi-independent pathways. These two different pathways may operate differentially depending on cell type or the developmental stage. In fact, the presence of α-TIP at the Golgi apparatus has been reported in pea cotyledon (Hinz et al., 1999; Hillmer et al., 2001), whereas Golgi-independent trafficking has been shown to occur in tobacco leaf protoplasts and culture cells (Gomez and Chrispeels, 1993; Jiang and Rogers, 1998). However, it is also possible that both pathways may operate within the same cell type. Interestingly, precursor accumulating vesicles, which are thought to be involved in delivery of cargoes from the ER to the PSV by a Golgi-independent pathway, also receive cargo molecules from the Golgi apparatus (Hara-Nishimura et al., 1998; Shimada et al., 2002).

MATERIALS AND METHODS

Growth of Plants

Common bean (*Phaseolus vulgaris*) and tobacco (*Nicotiana tabacum*) were grown in soil at 23°C in a greenhouse with a 16/8-h light/dark cycle. Arabidopsis was grown on B5 plates in a growth chamber at 23°C. Cotyledons and leaf tissues were harvested from plants and were immediately used for protoplast isolation.

Construction of Reporter Proteins

To generate HA-tagged α-TIP (accession no. X63551), PCR was carried out using two specific primers, 5′-CATAATGGCAACATCAGCT-3′ and 5′-TCAAGCATAATCTGGAACATCGTATGGATAGTAATCTTCAGGGGG-CAAG-3′. Subsequently, the PCR product was placed under the cauliflower mosaic virus 35S promoter and the nos terminator. To generate glycosylated α-TIP (α-TIP:gly:HA), the C-terminal region of phaseolin, including the N-glycosylation site (fragment I), was PCR amplified using 5′-CTTTTGGTC-CAGCGTTGGTGGAACTGAGCAAACATGCAAA-3′ and 5′-TGGTCATGC-CATCTCCATCCGGCCTTAGAATAGTAGTGTG-3′. Second, the N-terminal region of α-TIP (fragment II) was PCR amplified using 5′-TTAGCATGTTT-GCTCAGTTCCACCAACGCTGGACCAAAAG-3′ and 5′-TTTCAGAAA-

GAATGCTAACC-3′, and the C-terminal α-TIP region (fragment III) was PCR amplified using 5′-CACACTACTATTCTAAGGCCGGATGGAGAT-GGCATGACCA-3′ and 5′-GAACGATCGGGGAAATTC-3′. The fragments I and II were joined by PCR using 5′-TTTCAGAAAGAATGCTAACC-3′ and 5′-TGGTCATGCCATCTCCATCCGGCCTTAGAATAGTAGTGTG-3′ to generate fragment IV. Finally, fragments III and IV were joined by PCR using 5′-TTTCAGAAAGAATGCTAACC-3′ and 5′-GAACGATCGGGGA-AATTC-3′ to generate α-TIP:gly:HA. The nucleotide sequence of all the PCR products was confirmed by nucleotide sequencing. AtSec23 (accession no. AY122928) was PCR amplified using primers 5′-CTCGAGAGCTTCCAAC-GAATGGCGGAG-3′ and 5′-CAAATGGACTACTCAAGACTG-3′ and was tagged with the T7 epitope at the N terminus by placing the PCR product to pET-21a vector (Novagen, Madison, WI).

Transient Expression and in Vivo Targeting of Reporter Proteins

Plasmids were introduced into protoplasts prepared from leaf tissues of Arabidopsis, common bean, and tobacco by polyethylene glycol-mediated transformation (Hofte et al., 1991; Zhang et al., 1997; Jin et al., 2001). Expression of fusion constructs was monitored at various timepoints after transformation, as described previously (Jin et al., 2001).

Protein Extraction and Analysis of Endo-H

To prepare cell extracts, transformed protoplasts were first pelleted at 500 rpm for 5 min and the supernatant and pellet were collected separately. The pellet containing the protoplasts was resuspended in ice-cold homogenization buffer (25 mM HEPES, pH 7.7, 1 mM MgCl₂, 250 mM sucrose, and 1 mM dithiothreitol) supplemented with EDTA-free complete protease inhibitors cocktail (Roche Diagnostics, Mannheim, Germany). The protoplasts were then subjected to repeated freeze-thaw cycles followed by brief sonication for 3 s at the 50% output level three times. The medium fraction was processed to obtain proteins present in the medium. Bovine serum albumin was added to the supernatant at a concentration of 10 μg mL⁻¹. Proteins were then precipitated from the supernatant by adding a one-tenth volume of cold trichloroacetic acid. The protein pellet was washed with ice-cold 10% (w/v) trichloroacetic acid and was then dissolved in 0.1 N NaOH. Samples were analyzed by western blotting.

For chemical treatment, 25 μg mL⁻¹ BFA (10 mg mL⁻¹ stock solution in dimethyl sulfoxide; Sigma, St. Louis), 10 μg mL⁻¹ tunicamycin (10 mg mL⁻¹ stock solution in 10 mM NaOH; Sigma), or the equivalent amounts of respective solvents was added to the incubation medium right after transformation.

Endo-H digestion of phaseolin, α-TIP:HA, and α-TIP:gly:HA was performed as described previously (Frigerio et al., 2001). Samples were incubated with 1 mU of endo H (Roche Diagnostics) at 37°C for 1 h. Reaction was stopped by adding 5× SDS-PAGE loading buffer, and samples were then analyzed by SDS-PAGE and immunoblotting.

Immunohistochemistry

Protoplasts transformed with various constructs were resuspended in washing buffer (154 mM NaCl, 125 mM CaCl₂, 2.5 mM maltose, 5 mM KCl, and 10 mM HEPES, pH 7.4), and the cell suspension was spread onto positively charged slides (Fisher Scientific, Pittsburgh) and allowed to adhere for 1 h at room temperature. Cells were fixed in washing buffer containing 3% (w/v) paraformaldehyde for 1 h at room temperature (Frigerio et al., 2001). Cells were then permeabilized by washing three times with buffer (10 mM Tris-HCl, pH 7.4, 0.9% [w/v] NaCl, 0.25% [w/v] gelatin, 0.02% [w/v] SDS, and 0.1% [w/v] Triton X-100 [TSW]) for 30 min at room temperature. After three final washes in TSW, cells were stained with primary antibodies such as antiphaseolin antibody (Frigerio et al., 2001), anti-α-TIP antibody (Jauh et al., 1998; Jiang et al., 1998), or anti-HA antibody (3F10; Roche Diagnostics) for 16 h at 4°C. After binding of the primary antibody, cells were washed three times with TSW buffer and stained with secondary antibodies such as TRITC-labeled anti-rat IgG, FITC-labeled anti-rabbit IgG antibody, or TRITC-labeled anti-rabbit IgG antibody (Zymed, San Francisco) for 16 h at 4°C. Samples were examined under a fluorescent microscope, as described previously (Jin et al., 2001).

Protein Fractionation and Western-Blot Analysis

To prepare cell extracts from protoplasts, transformed protoplasts were lysed by repeated freeze-thaw cycles and were then centrifuged at 7,000g at 4°C for 5 min in a microfuge to remove cell debris (Jin et al., 2001). Western-blot analysis was carried out using anti-GFP (Clontech, Palo Alto, CA), anti-T7 (Novagen, Madison, WI) antiphaseolin, or anti-α-TIP antibody as described previously (Jin et al., 2001).

RT/PCR Analysis

Total RNA was prepared from Arabidopsis seeds imbibed for 3 d, or leaf tissues of 3-week-old plants using Trizol LS reagent (Invitrogen, Carlsbad, CA) following the manufacturer's instructions. cDNA was synthesized using 1 μg of total RNA with Superscript II-RNase H$^-$ reverse transcriptase (Invitrogen). Primers were 5'-ATGGCAACATCAGCTCGTAGA-3' and 5'-GTGGGTAGGTGGTTCGGTGGG-3' for α-TIP, and 5'-ATGCCGATCAG-AAACATCGCC-3' and 5'-GAGCTGCTCGTGTGTGGTGTT-3' for γ-TIP. PCR products were confirmed by nucleotide sequencing.

ACKNOWLEDGMENTS

LITERATURE CITED

Aubert S, Gout E, Bligny R, Marty-Mazars D, Barrieu F, Alabouvette J, Marty F, Douce R (1996) Ultrastructural and biochemical characterization of autophagy in higher plant cells subjected to carbon deprivation: control by the supply of mitochondria with respiratory substrates. J Cell Biol **133**: 1251–1263

Bagga S, Adams H, Kemp JD, Sengupta-Gopalan C (1995) Accumulation of the 15-kD zein in novel protein bodies in transgenic tobacco. Plant Physiol **107**: 13–23

Bassham DC, Raikhel NV (2000) Unique features of the plant vacuolar sorting machinery. Curr Opin Cell Biol **12**: 491–495

Batoko H, Zheng HQ, Hawes C, Moore I (2000) A rab1 GTPase is required for transport between the endoplasmic reticulum and Golgi apparatus and for normal Golgi movement in plants. Plant Cell **12**: 2201–2218

Boevink P, Martin B, Oparka K, Santa Cruz S, Hawes C (1999) Transport of virally expressed green fluorescent protein through the secretory pathway in tobacco leaves is inhibited by cold shock and brefeldin A. Planta **208**: 392–400

Bollini R, Chrispeels MJ (1978) Characterization and subcellular localization of vicilin and phytohemagglutinin, the two major reserve proteins of *Phaseolus vulgaris* L. Planta **142**: 291–298

Chrispeels MJ (1983) The Golgi apparatus mediates the transport of phytohaemagglutinin to the protein bodies in bean cotyledons. Planta **158**: 140–151

Di Sansebastiano GP, Paris N, Marc-Martin S, Neuhaus JM (2001) Regeneration of a lytic central vacuole and of neutral peripheral vacuoles can be visualized by green fluorescent proteins targeted to either type of vacuoles. Plant Physiol **126**: 78–86

Frigerio L, de Virgilio M, Prada A, Faoro F, Vitale A (1998) Sorting of phaseolin to the vacuole is saturable and requires a short C-terminal peptide. Plant Cell **10**: 1031–1042

Frigerio L, Pastres A, Prada A, Vitale A (2001) Influence of KDEL on the fate of trimeric or assembly-defective phaseolin: selective use of an alternative route to vacuoles. Plant Cell **13**: 1109–1126

Gomez L, Chrispeels MJ (1993) Tonoplast and soluble vacuolar proteins are targeted by different mechanisms. Plant Cell **5**: 1113–1124

Hara-Nishimura I, Shimada T, Hatano K, Takeuchi Y, Nishimura M (1998) Transport of storage proteins to protein storage vacuoles is mediated by large precursor-accumulating vesicles. Plant Cell **10**: 825–836

Herman EM, Larkins BA (1999) Protein storage bodies and vacuoles. Plant Cell **11**: 601–613

Hillmer S, Movafeghi A, Robinson DG, Hinz G (2001) Vacuolar storage proteins are sorted in the cis-cisternae of the pea cotyledon Golgi apparatus. J Cell Biol **152**: 41–50

Hinz G, Hillmer S, Baumer M, Hohl I (1999) Vacuolar storage proteins and the putative vacuolar sorting receptor BP-80 exit the Golgi apparatus of developing pea cotyledons in different transport vesicles. Plant Cell **11**: 1509–1524

Höfte H, Faye L, Dickinson C, Herman EH, Chrispeels MJ (1991) The protein body proteins phytohemagglutinin and tonoplast intrinsic protein are targeted to vacuoles in leaves of transgenic tobacco. Planta **184**: 431–437

Hoh B, Hinz G, Jeong B-K, Robinson DG (1995) Protein storage vacuoles form de novo during pea cotyledon development. J Cell Sci **108**: 299–310

Holkeri H, Vitale A (2001) Vacuolar sorting determinants within a plant storage protein trimer act cumulatively. Traffic **2**: 737–741

Jauh GY, Fischer AM, Grimes HD, Ryan CA Jr, Rogers JC (1998) δ-Tonoplast intrinsic protein defines unique plant vacuole functions. Proc Natl Acad Sci USA **95**: 12995–12999

Jauh GY, Phillips TE, Rogers JC (1999) Tonoplast intrinsic protein isoforms as markers for vacuolar functions. Plant Cell **11**: 1867–1882

Jiang L, Phillips TE, Hamm CA, Drozdowicz YM, Rea PA, Maeshima M, Rogers SW, Rogers JC (2001) The protein storage vacuole: a unique compound organelle. J Cell Biol **155**: 991–1002

Jiang L, Phillips TE, Rogers SW, Rogers JC (2000) Biogenesis of the protein storage vacuole crystalloid. J Cell Biol **150**: 755–770

Jiang L, Rogers JC (1998) Integral membrane protein sorting to vacuoles in plant cells: evidence for two pathways. J Cell Biol **143**: 1183–1199

Jin JB, Kim YA, Kim SJ, Lee SH, Kim DH, Cheong GW, Hwang I (2001) A new dynamin-like protein, ADL6, is involved in trafficking from the trans-Golgi network to the central vacuole in Arabidopsis. Plant Cell **13**: 1511–1526

Johnson KD, Herman EM, Chrispeels MJ (1989) An abundant, highly conserved tonoplast protein in seeds. Plant Physiol **91**: 1006–1013

Kim DH, Eu YJ, Yoo CM, Kim YW, Pih KT, Jin JB, Kim SJ, Stenmark H, Hwang I (2001) Trafficking of phosphatidylinositol 3-phosphate from the trans-Golgi network to the lumen of the central vacuole in plant cells. Plant Cell **13**: 287–301

Lee MH, Min MK, Lee YJ, Jin JB, Shin DH, Kim DH, Lee KH, Hwang I (2002) ADP-ribosylation factor 1 of Arabidopsis plays a critical role in intracellular trafficking and maintenance of endoplasmic reticulum morphology in Arabidopsis. Plant Physiol **129**: 1507–1520

Levanony H, Rubin R, Altschuler Y, Galili G (1992) Evidence for a novel route of wheat storage proteins to vacuoles. J Cell Biol **119**: 1117–1128

Marty F (1999) Plant vacuoles. Plant Cell **11**: 587–599

Movafeghi A, Happel N, Pimpl P, Tai GH, Robinson DG (1999) Arabidopsis Sec21p and Sec23p homologs: probable coat proteins of plant COP-coated vesicles. Plant Physiol **119**: 1437–1446

Muntz K (1998) Deposition of storage proteins. Plant Mol Biol **38**: 77–99

Nebenfuhr A, Ritzenthaler C, Robinson DG (2002) Brefeldin A: deciphering an enigmatic inhibitor of secretion. Plant Physiol **130**: 1102–1108

Neuhaus JM, Rogers JC (1998) Sorting of proteins to vacuoles in plant cells. Plant Mol Biol **38**: 127–144

Paris N, Stanley CM, Jones RL, Rogers JC (1996) Plant cells contain two functionally distinct vacuolar compartments. Cell **85**: 563–572

Pedrazzini E, Giovinazzo G, Bielli A, de Virgilio M, Frigerio L, Pesca M, Faoro F, Bollini R, Ceriotti A, Vitale A (1997) Protein quality control along the route to the plant vacuole. Plant Cell **9**: 1869–1880

Phillipson B, Pimpl P, Crofts AJ, Movafeghi A, Taylor JP, Robinson DG, Denecke J (2001) Secretory bulk flow of soluble proteins is efficient and COPII dependent. Plant Cell **13**: 2005–2020

Ritzenthaler C, Nebenfuhr A, Movafeghi A, Stussi-Garaud C, Behnia L, Pimpl P, Staehelin LA, Robinson DG (2002) Reevaluation of the effects of brefeldin A on plant cells using tobacco Bright Yellow 2 cells expressing Golgi-targeted green fluorescent protein and COPI antisera. Plant Cell **14**: 237–261

Saalbach G, Jung R, Kunze G, Saalbach I, Adler K, Muntz K (1991) Different legumin protein domains act as vacuolar targeting signals. Plant Cell **3**: 695–708

Sanderfoot AA, Kovaleva V, Bassham DC, Raikhel NV (2001) Interactions between syntaxins identify at least five SNARE complexes within the Golgi/prevacuolar system of the Arabidopsis cell. Mol Biol Cell **12:** 3733–3743

Shimada T, Watanabe E, Tamura K, Hayashi Y, Nishimura M, Hara-Nishimura I (2002) A vacuolar sorting receptor PV72 on the membrane of vesicles that accumulate precursors of seed storage proteins (PAC vesicles). Plant Cell Physiol **43:** 1086–1095

Sohn EJ, Kim ES, Zhao M, Kim SJ, Kim H, Kim YW, Lee YJ, Hillmer S, Sohn U, Jiang L et al. (2003) Rha1, an Arabidopsis Rab5 homolog, plays a critical role in the vacuolar trafficking of soluble cargo proteins. Plant Cell **15:** 1057–1070

Swanson SJ, Bethke PC, Jones RL (1998) Barley aleurone cells contain two types of vacuoles: characterization of lytic organelles using fluorescent probes. Plant Cell **10:** 685–698

Takeuchi M, Ueda T, Sato K, Abe H, Nagata T, Nakano A (2000) A dominant negative mutant of sar1 GTPase inhibits protein transport from the endoplasmic reticulum to the Golgi apparatus in tobacco and Arabidopsis cultured cells. Plant J **23:** 517–525

Tani K, Mizoguchi T, Iwamatsu A, Hatsuzawa K, Tagaya M (1999) p125 is a novel mammalian Sec23p-interacting protein with structural similarity to phospholipid-modifying proteins. J Biol Chem **274:** 20505–20512

Törmäkangas K, Hadlington JL, Pimpl P, Hillmer S, Brandizzi F, Teeri TH, Denecke J (2001) A vacuolar sorting domain may also influence the way in which proteins leave the endoplasmic reticulum. Plant Cell **13:** 2021–2032

Toyooka K, Okamoto T, Minamikawa T (2000) Mass transport of proform of a KDEL-tailed cysteine proteinase (SH-EP) to protein storage vacuoles by endoplasmic reticulum-derived vesicle is involved in protein mobilization in germinating seeds. J Cell Biol **148:** 453–464

Tranbarger TJ, Franceschi VR, Hildebrand DF, Grimes HD (1991) The soybean 94-kilodalton vegetative storage protein is a lipooxygenase that is localized in paraveinal mesophyll cell vacuoles. Plant Cell **3:** 973–987

Vitale A, Raikhel NV (1999) What do proteins need to reach different vacuoles? Trends Plant Sci **4:** 149–155

Zhang WH, Walker NA, Tyerman SD, Patrick JW (1997) Mechanisms of solute efflux from seed coats: whole cell K^+ currents in transfer cell protoplasts derived coats of developing seeds of *Vicia faba* L. J Exp Bot **48:** 1565–1572